

Effective field theory of pairing rotations

T. Papenbrock 

*Department of Physics and Astronomy, University of Tennessee, Knoxville, Tennessee 37996, USA
and Physics Division, Oak Ridge National Laboratory, Oak Ridge, Tennessee 37831, USA*



(Received 26 February 2022; accepted 6 April 2022; published 22 April 2022)

Pairing rotations are the low-energy excitations of finite superfluid systems, connecting systems that differ in their number of Cooper pairs. This paper presents a model-independent derivation of pairing rotations within an effective theory that exploits the emergent breaking of U(1) phase symmetries. The symmetries are realized nonlinearly and the Nambu-Goldstone modes depend only on time because the system is finite. Semimagic nuclei exhibit pairing rotational bands while the pairing spectrum becomes an elliptical paraboloid for open-shell nuclei. Model-independent relations between double charge-exchange reactions and α particle capture or knockout in open-shell nuclei are in analogy to the pair transfer reactions in a single superfluid. Odd semimagic nuclei are described by coupling a fermion to the superfluid. The leading-order theories reproduce data for pairing rotational bands within uncertainty estimates.

DOI: [10.1103/PhysRevC.105.044322](https://doi.org/10.1103/PhysRevC.105.044322)

I. INTRODUCTION

Atomic nuclei are finite superconductors. Hallmarks of nuclear pairing are excitation gaps in even-even nuclei [1], reduced moments of inertia due to superfluidity [2], odd-even staggerings in many observables, and pairing vibrations [3] and rotations [4–7] (see Ref. [8] for an overview). Pairing rotational spectra are the analog to rotational bands in deformed nuclei; they are quadratic in the difference of Cooper pairs and are associated with the Nambu-Goldstone mode of a broken U(1) phase symmetry [9–11]. They explain why two-nucleon transfer is enhanced between nuclei within a pairing-rotational band [7,12–16]. Pairing rotational modes have been studied via pairing models, see, e.g., Refs. [6,7,17,18], and in Hartree-Fock-Bogoliubov [19,20] and relativistic mean-field computations [21].

In this paper I revisit pairing rotations in the framework of effective field theory [22–30]. This brings simplicity and model independence to an old subject. The approach requires one to be conscious about the breakdown scale, and the power counting allows one to estimate or quantify [31,32] uncertainties. Open-shell nuclei are described as two interacting superfluids starting from the most general Lagrangian compatible with the symmetry breaking. As we will see, the model-independent approach yields relations between double charge-exchange reactions and two-nucleon transfer, and these can be tested experimentally.

The approach presented in this work differs from that by Furnstahl *et al.* [25]. That work proposed an effective field theory for dilute Fermi systems. Here I merely exploit the dynamics of Nambu-Goldstone modes corresponding to the emergent breaking of phase symmetries in finite systems. Then quantum field theory reduces to quantum mechanics [33] and a fermion only appears in odd systems.

This paper is organized as follows: Section II present the effective field theory for even and odd semimagic nuclei, respectively. The theory for open-shell even-even nuclei is derived in Sec. III. The theory is confronted with data in Sec. IV. The summary in Sec. V discusses the main results.

II. EFFECTIVE THEORY FOR A SINGLE SUPERFLUID

A. Even semimagic nuclei

1. Leading-order Hamiltonian

I consider a finite superfluid of a single fermion species with spin 1/2 and assume that all fermions are in Cooper pairs. Examples are even isotopes of tin or lead, or even isotones with neutron number $N = 82$. The corresponding nuclear ground states must be invariant under U(1) phase transformations which are generated by

$$g(\alpha) = e^{i\alpha\hat{n}}. \quad (1)$$

Here α is the phase angle and \hat{n} is the operator that yields the number of pairs. A finite system displays emergent rather than spontaneous symmetry breaking [34]. Nevertheless, one can follow the standard approach to spontaneous symmetry breaking via nonlinear realizations [35–38], and the Nambu-Goldstone mode parametrizes the coset $U(1)/1 \sim U(1)$ of the broken symmetry. For finite systems, however, a tremendous simplification occurs because the Nambu-Goldstone “field” $\alpha = \alpha(t)$ depends only on time [33,39], and quantum field theory thus reduces to quantum mechanics. In the present case, the phase velocity

$$\dot{\alpha} \equiv \partial_t \alpha \quad (2)$$

is the only quantity that can enter the Lagrangian.

The leading-order Lagrangian then becomes

$$L_{\text{LO}} = \frac{a}{2}\dot{\alpha}^2 + n_0\dot{\alpha}. \quad (3)$$

Here, a and n_0 are low-energy constants. The constant a is akin to a mass term while n_0 is a constant gauge potential. A Legendre transformation yields the Hamiltonian

$$H_{\text{LO}} = \frac{1}{2a}(p_\alpha - n_0)^2. \quad (4)$$

Here,

$$p_\alpha \equiv \frac{\partial L}{\partial \dot{\alpha}} \quad (5)$$

is the canonical momentum. Clearly, p_α is a constant of motion. The interpretation of p_α as the number of pairs n becomes clear when considering phase transformations $g(\beta)g(\alpha) = g(\alpha + \beta)$. The phase α changes to $\alpha + \beta$ and this is a nonlinear realization of the phase symmetry. Applying Noether's theorem to infinitesimal phase transformations then yields that p_α is conserved and therefore must be identified with the number of pairs.

One quantizes the Hamiltonian (4) as usual via

$$p_\alpha \rightarrow \hat{p}_\alpha = -i\partial_\alpha, \quad (6)$$

(and of course also identifies the pair number operator as $\hat{n} = -i\partial_\alpha$.) Thus, the Hamiltonian is

$$\begin{aligned} H &= \frac{1}{2a}(-i\partial_\alpha - n_0)^2 \\ &= \frac{1}{2a}(\hat{n} - n_0)^2. \end{aligned} \quad (7)$$

Requiring that the wave function $\psi(\alpha)$ is single-valued under gauge transformations $\psi(\alpha) \rightarrow \psi'(\alpha) = e^{i\lambda\alpha}\psi(\alpha)$ with constant λ then shows that n_0 must be an integer. Eigenfunctions are

$$\psi_n(\alpha) = \langle \alpha | n \rangle = \frac{1}{\sqrt{2\pi}} e^{in\alpha}, \quad (8)$$

and these describe a system of n pairs. The corresponding energies

$$\varepsilon_n = \frac{1}{2a}(n - n_0)^2 \quad (9)$$

are in a pairing rotational band.

Let us consider time-reversal invariance. The pair-number operator $\hat{n} = \hat{p}_\alpha$ is even under time reversal. This implies that the phase α is odd. As $\dot{\alpha}$ is even under time reversal, higher-order contributions to the effective theory can also contain odd powers of the phase velocity. Under time reversal, the eigenfunction $\psi_n(\alpha) \rightarrow \psi_n(-\alpha) = \psi_n^*(\alpha) = \psi_{-n}(\alpha)$. Formally, one could admit negative pair numbers n (and negative n_0), and the spectrum is invariant under this change. In this case, one would interpret n as the number of hole pairs.

Besides the number operator \hat{n} , the other operator of interest is the pair-removal operator \hat{P} with matrix elements

$$\langle \alpha' | \hat{P} | \alpha \rangle = P_0 e^{-i\alpha} \delta(\alpha' - \alpha). \quad (10)$$

Here, P_0 is a constant that denotes the overall strength. Clearly $\hat{P}|n\rangle = P_0|n-1\rangle$, and $\hat{P}^\dagger|n\rangle = P_0^*|n+1\rangle$. The effective theory then predicts that $\langle n+1 | \hat{P}^\dagger | n \rangle = P_0^*$, i.e., pair transfer within the nuclei of a pairing rotational band is independent of the number of pairs in a given nucleus. This hallmark of pairing rotations has been confirmed experimentally in two-nucleon transfer reactions, see Refs. [7,12,14].

Pairing vibrations fall outside the scope of the effective theory presented in this paper. To include them, one would need to add another degree of freedom that accounts for two-quasiparticle excitations at fixed pair number: Simple models of pairing vibrations consist of two j shells (while pairing rotations result already from a single j shell) [8].

2. Power counting

Effective theories exploit a separation of energy scales and organize the Hamiltonian by a power counting. In the present case, the Lagrangian (3) is postulated to be of the low-energy scale ξ . One thus assigns the scalings

$$a \sim \xi^{-1}, \quad (11)$$

$$\dot{\alpha} \sim n_0 \xi, \quad (12)$$

and it is implied that the two terms of the Lagrangian (3) combine (or cancel) to yield the low-energy scale ξ . Then the Hamiltonian (4) is also of order ξ , but its size is really about $\xi(n - n_0)^2$, which quickly can become large. Below we will see that $1/(2a) \approx 0.4$ MeV for tin ($Z = 50$) isotopes, 0.25 MeV for lead isotopes ($Z = 82$), and 1.0 MeV for $N = 82$ isotones. The comparison of tin and lead isotopes on the one hand and the $N = 82$ isotones on the other hand also shows that neutron pairing is associated with a lower energy scale than proton pairing.

In effective field theories, corrections to the leading-order are due to neglected physics at high energy. This introduces the breakdown energy scale Λ_b , and a corresponding breakdown pair number, $n_b = \sqrt{2a\Lambda_b}$ via Eq. (9). I will thus assume that shell closures determine the breakdown of pairing. Then $|n - n_0|$ cannot be larger than the number of pairs in a major shell, i.e., $n_b \approx 15$ or 20 in heavy nuclei. This would suggest that $\Lambda_b/\xi \approx n_b^2 \gg 1$, and the scale separation should be large.

The subleading correction to the Lagrangian (3) contains the term $\dot{\alpha}^3$, and at next-to-leading order the Hamiltonian can be written as

$$H_{\text{NLO}} = H_{\text{LO}} + \frac{g}{3}(\hat{n} - n_0)^3. \quad (13)$$

Here, the factor 1/3 is introduced for convenience. Energies are obtained by replacing the number operator with its eigenvalues, i.e.

$$\tilde{\varepsilon}_n = \frac{1}{2a}(n - n_0)^2 + \frac{g}{3}(n - n_0)^3. \quad (14)$$

An estimate for the low-energy constant g results from the assumption that—at the breakdown scale—the correction proportional to g is clearly visible, i.e., it is as large as the leading-order energy spacing $|E_{n_b+1} - E_{n_b}| \approx |n_b - n_0|/a$. This yields the estimate $|g| \approx 3/[a(n_b - n_0)^2]$. To make

this estimate independent of n_0 one replaces $(n_b - n_0)^2$ by its average $n_b^2/3$, taken over the shell. This then yields

$$|g| \approx \frac{9}{an_b^2}, \quad (15)$$

and the uncertainty estimate for leading-order results is

$$\Delta \varepsilon_n \approx \frac{3|n - n_0|^3}{an_b^2}. \quad (16)$$

Below the breakdown energy, the term proportional to g is then suppressed by a factor $1/n_b \ll 1$ compared with the leading term.

It is clear how to generalize this approach to even higher orders: The Lagrangian is expanded in powers of the phase velocity $\dot{\alpha}$, and the Hamiltonian becomes an expansion in powers of $(\hat{n} - n_0)$; subsequent orders are suppressed by increasing factors of $\sqrt{\xi/\Lambda_b} \sim n_b^{-1}$.

The assumptions underlying the power counting can be tested by extracting the low-energy coefficients $(2a)^{-1}$ and g from data. In analogy to rotations of deformed nuclei, one can also think about subleading corrections in the framework of a variable moment of inertia [40]. This introduces the n -dependent pairing rotational constant as

$$\frac{1}{2} \frac{\partial^2 \varepsilon_n}{\partial n^2} = \frac{1}{2a} + g(n - n_0). \quad (17)$$

This expression will be used below to extract g from data.

B. Odd semimagic nuclei

Pairing rotations in odd systems were previously considered in Ref. [41] using a BCS state within a pairing model. Within the effective theory they can be described as a spin-1/2 fermion coupled to the superfluid.

The Lagrangian is

$$L = \frac{a}{2} \dot{\alpha}^2 + n_0 \dot{\alpha} + L_\chi + L_{\text{int}}. \quad (18)$$

The fermion Lagrangian is

$$L_\chi = \int d^3\mathbf{r} \hat{\chi}^\dagger(\mathbf{r}) \left(i\partial_t + \frac{\hbar^2 \Delta_{\mathbf{r}}}{2m} - V \right) \hat{\chi}(\mathbf{r}), \quad (19)$$

and the interaction L_{int} will be specified shortly. Here, I have introduced the two-component fermion field

$$\hat{\chi}(\mathbf{r}) = \begin{pmatrix} \hat{\chi}_{+\frac{1}{2}}(\mathbf{r}) \\ \hat{\chi}_{-\frac{1}{2}}(\mathbf{r}) \end{pmatrix}, \quad (20)$$

and its adjoint. The operators $\hat{\chi}_s^\dagger(\mathbf{r})$ and $\hat{\chi}_s(\mathbf{r})$ create and annihilate a fermion with spin projection $s = \pm 1/2$ at the position \mathbf{r} , respectively. They fulfill the usual anticommutation relations. In Eq. (19) the potential is denoted as V and the fermion's mass as m . I neglected fermion-fermion interactions because the interest is in a single fermion coupled to a superfluid.

The fermion-pair number operator is

$$\hat{n}_\chi = \frac{1}{2} \int d^3\mathbf{r} \hat{\chi}^\dagger(\mathbf{r}) \hat{\chi}(\mathbf{r}), \quad (21)$$

and this operator couples the fermion to the superfluid via

$$L_{\text{int}} = -\hat{n}_\chi \dot{\alpha}. \quad (22)$$

The superfluid-fermion interaction (22) is so simple because (i) the coupling of the fermion to the superfluid must be via the phase velocity (as one deals with a Nambu-Goldstone mode) and (ii) it can only happen in gauge space, i.e., via the fermion-pair number operator (21). The sign is chosen for convenience. As \hat{n}_χ has half integer eigenvalues, the wave function $\psi(\alpha)$ of the superfluid is double-valued, i.e., it goes over into itself after a rotation by 4π in gauge space. (This is in analogy to Wigner D functions at half-integer angular momentum.) Furthermore, the choice of the coupling (22) ensures that the wave function of the superfluid remains double-valued under gauge transformations $\psi \rightarrow e^{i\lambda\alpha} \psi$.

The canonical momentum of the superfluid is $p_\alpha = \frac{\delta L}{\delta \dot{\alpha}}$, and the behavior of the superfluid under phase transformations is as before. Under phase transformations with an infinitesimal angle $\delta\beta$, the fermion field changes by

$$e^{i\delta\beta\hat{n}_\chi} \hat{\chi}_s(\mathbf{r}) e^{-i\delta\beta\hat{n}_\chi} = \hat{\chi}_s(\mathbf{r}) - i\delta\beta \hat{\chi}_s(\mathbf{r}). \quad (23)$$

Introducing the fermion canonical momenta

$$\hat{\Pi}_s(\mathbf{r}) \equiv \frac{\delta L}{\delta \partial_t \chi_s(\mathbf{r})} = i\hat{\chi}_s^\dagger(\mathbf{r}) \quad (24)$$

and applying Noether's theorem to the coupled system then shows that the total number of pairs,

$$\hat{n}_{\text{tot}} = p_\alpha + \hat{n}_\chi, \quad (25)$$

is conserved under phase rotations. This is as expected. After the quantization (6) the eigenstates of \hat{n}_{tot} are products of a superfluid state $|n\rangle$ with n pairs and a fermion state. I denote the latter as $|qj j_z\rangle$ where j denotes the fermion's total angular momentum, j_z denotes its projection onto an arbitrary axis, and q accounts for any other quantum numbers. Thus

$$\hat{n}_{\text{tot}} |n\rangle |qj j_z\rangle = (n + \frac{1}{2}) |n\rangle |qj j_z\rangle, \quad (26)$$

with half integer numbers of pairs $n_{\text{tot}} = n + 1/2$.

A Legendre transform yields the Hamiltonian

$$\begin{aligned} \hat{H} &= \frac{1}{2a} (-i\partial_\alpha + \hat{n}_\chi - n_0)^2 + \hat{H}_\chi \\ &= \frac{1}{2a} (\hat{n}_{\text{tot}} - n_0)^2 + \hat{H}_\chi, \end{aligned} \quad (27)$$

with

$$\hat{H}_\chi = \int d^3\mathbf{r} \hat{\chi}^\dagger(\mathbf{r}) \left(-\frac{\hbar^2 \Delta_{\mathbf{r}}}{2m} + V \right) \hat{\chi}(\mathbf{r}). \quad (28)$$

The eigenstates (26) of the total pair-number operator are also eigenstates of the Hamiltonian (27). Using

$$\hat{H}_\chi |qj j_z\rangle = e_{qj} |qj j_z\rangle \quad (29)$$

yields the spectrum

$$\varepsilon_{n_{\text{tot}} q j} = \frac{1}{2a} (n_{\text{tot}} - n_0)^2 + e_{qj}. \quad (30)$$

This shows that one also has pairing rotational bands in odd-mass nuclei. These connect states that differ by the number of

pairs but have equal spin and parity. In contrast with pairing-rotational bands in even-even nuclei, these are not necessarily ground states. The Hamiltonian (27) must reduce to Eq. (7) when acting onto the fermion vacuum. Thus, n_0 is an integer. Except for the uninteresting constant e_{qj} the pairing rotational bands in odd and even nuclei have the same parabolic form. As in the case of even isotopes, the theory for odd nuclei also predicts that pair transfer and removal is equal in strength for states of a pairing rotational band. Subleading corrections are similar to those for even nuclei, i.e., one has an expansion of the Hamiltonian in powers of $(n_{\text{tot}} - n_0)$.

C. Adjustment of low-energy constants

The spectra (9) and (30) relate superfluid systems in the vicinity of integer n_0 pairs to each other. Before one can apply the effective theory of pairing rotations to nuclei, however, the dominant energy contributions to nuclear states must be included. These consist of an overall constant and a term linear in the number of pairs.

Let us consider even nuclei first. Adding the contributions $E_{n_0} + S(\hat{n} - n_0)$ to the Hamiltonian (7) yields the energy spectrum

$$E_n = E_{n_0} - S_{n_0}(n - n_0) + \varepsilon_n. \quad (31)$$

Here, E_{n_0} is the ground-state energy of the nucleus with n_0 pairs, and S_{n_0} denotes the pair removal energy, and ε_n is from Eq. (9). As $E_{n_0} \approx -8A$ MeV for a nucleus with mass number A and $S_{n_0} \approx 16$ MeV for heavy nuclei, the pairing rotation energies ε_n only yield a small correction [except when $(n - n_0)^2 \gg 1$] because the low-energy scale ξ is much smaller than S_{n_0} .

The expansion (31) presents a challenge for theories about pairing [40]. One could generally argue that the ground-state energy E_n can be expanded around n_0 in powers of $(n - n_0)$. Then, the leading-order theory for pairing would be just one contribution to the quadratic term, and other contributions are hard to pin down without a microscopic theory. However, the leading-order effective theory predicts that the pairing rotational constant a in Eq. (9) does not depend on which nucleus (identified by the number of pairs n_0) the band is centered. Within the effective theory, any variation of a must be attributed to subleading corrections, see Eq. (17). Thus, when exploring pairing rotational bands, one can vary n_0 and find out if any observed variation of a is consistent with the size of subleading contributions.

This suggests the following approach. I will assume that pairing yields the dominant quadratic term in the energy expansion and adjust the low-energy constants E_{n_0} , S_{n_0} , and a to the binding energies of the nuclei with n_0 and $n_0 \pm 1$ pairs via

$$\begin{aligned} S_{n_0} &= \frac{1}{2}(E_{n_0-1} - E_{n_0+1}), \\ a^{-1} &= E_{n_0+1} - 2E_{n_0} + E_{n_0-1}. \end{aligned} \quad (32)$$

Clearly, S_{n_0} is the average of two two-nucleon separation energies, while the rotational constant is a three-point difference of even nuclei. When adjusting a this way it becomes an n_0 -dependent quantity, and the variations of a with n_0 indicate the size of subleading corrections.

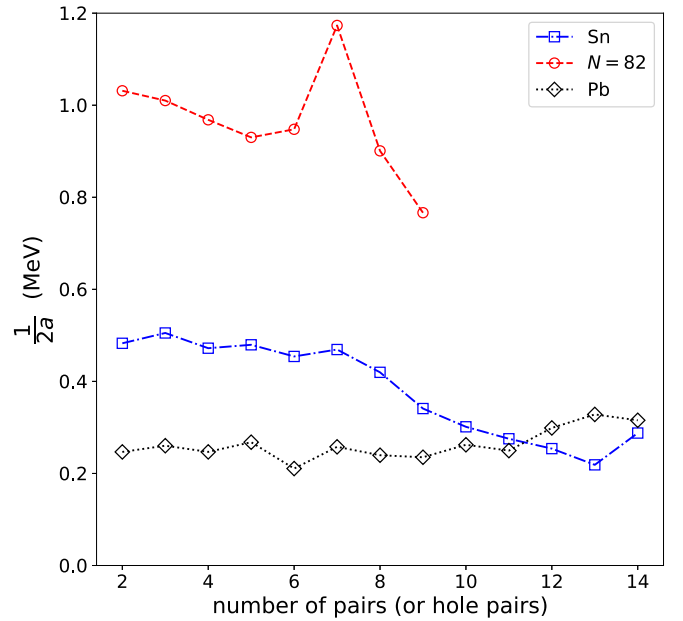


FIG. 1. Pairing rotational constants for even isotopes of tin (as a function of pairs above neutron number $N = 50$), of $N = 82$ isotones (as a function of pairs above proton number $N = 50$) and lead (as a function of pair holes below the neutron number $N = 126$).

Figure 1 shows the pairing rotational constant $(2a)^{-1}$, computed via Eq. (32), for even isotopes of tin (as a function of pairs above neutron number $N = 50$), of $N = 82$ isotones (as a function of pairs above proton number $N = 50$) and lead (as a function of pair holes below the neutron number $N = 126$). Clearly, the pairing rotational constant is approximately independent of n_0 for isotopes of lead while the $N = 82$ isotones and the isotopes of tin exhibit more variations. This suggests that higher-order corrections are significant in those nuclei. One also sees that the variations are not smooth as the number of pairs (or pair holes in lead) changes. This suggests that the (smooth) subleading contributions discussed in Sec. II A 2 are only part of the corrections beyond quadratic order. The nonsmooth fluctuations are outside the scope of the effective theory. They also prevent one from adjusting subleading low-energy constants locally, i.e., in a vicinity of a given n_0 .

Therefore, I consider global adjustments of g in Eq. (14) and check the power counting. The average slopes of the lines in Fig. 1 are small compared with the rotational constants, and this suggests that the smooth subleading correction could be systematic. Using Eq. (17) one identifies the average slope as g . Table I presents the average values of the rotational constant $(2a)^{-1}$ and g for the tin and lead isotopes and the $N = 82$ isotones. Also shown is the maximum number of pairs for the major shell corresponding to the nuclei of interest, and the estimate $3/(\langle a \rangle n_0^2)$ from Eq. (15) for the size of the coupling g . The theoretical estimates correctly identify the scale of $\langle |g| \rangle$ (they are about twice of what was extracted from data), and this gives one confidence in the power counting proposed in Sec. II A 2.

Thus, the uncertainty estimate (16) is expected to capture the smooth corrections to the leading-order pairing rotational

TABLE I. Average values of pairing rotational constants $(2a)^{-1}$ and the absolute average scale $|\langle g \rangle|$ for subleading correction (both in MeV) for isotopes of tin and lead, and $N = 82$ isotones. Also shown are the maximum number of pairs n_b in the relevant major shell, and—in the last column—the estimate (15) for the size of the low-energy constant g (in MeV).

	$\langle(2a)^{-1}\rangle$	$ \langle g \rangle $	n_b	$9/(\langle a \rangle n_b^2)$
Sn	0.38	0.016	16	0.027
Pb	0.26	0.0057	22	0.0097
$N = 82$	0.97	0.038	16	0.068

bands. In what follows I assume that pairing yields the dominant quadratic contribution to the expansion (31), limit the discussion to the leading-order theory, and use the uncertainty estimate (16).

For odd nuclei, one expands the pairing rotational contribution as $(n_{\text{tot}} - n_0)^2 = (n_{\text{tot}} - n_0 - 1/2)^2 + [n_{\text{tot}} - n_0 - 1/4]$. The constant and linear terms $[n_{\text{tot}} - n_0 - 1/4]$ can then be absorbed in an expansion of the energy (31). Thus, I employ Eqs. (31) and (32) for even nuclei (by using integer n_0) and for odd nuclei (by using half integer n_0). Inspection shows that the pairing rotational constants for the odd nuclei are close to their even neighbors. This allows me to use the data in Table I also for uncertainty estimates in odd nuclei.

III. EFFECTIVE THEORY FOR TWO SUPERFLUIDS

A. Even-even nuclei

In heavy open-shell nuclei, neutrons form isovector pairs and so do protons, and both superfluids interact. In what follows, I will not consider proton-neutron pairing but will include interactions between proton and neutron pairs. The effective theory is based on the emergent symmetry breaking from $U(1) \times U(1) \rightarrow 1$, and the coset is isomorph to $U(1) \times U(1)$. The phases $\alpha(t)$ and $\beta(t)$ denote the Nambu-Goldstone modes corresponding to neutron and proton pairs, respectively. The most general Lagrangian up to quadratic terms in phase velocities is

$$L = \frac{1}{2}(\dot{\alpha}, \dot{\beta})\hat{M}\begin{pmatrix} \dot{\alpha} \\ \dot{\beta} \end{pmatrix} + (n_0, z_0)\begin{pmatrix} \dot{\alpha} \\ \dot{\beta} \end{pmatrix}. \quad (33)$$

Here, n_0 and z_0 are low-energy constants and \hat{M} is a symmetric 2×2 “mass” matrix with three parameters, and I employed a matrix-vector notation. The off-diagonal elements of \hat{M} introduce an interaction between the two superfluids. Introducing the canonical momenta $p_\alpha \equiv \frac{\partial L}{\partial \dot{\alpha}}$ and $p_\beta \equiv \frac{\partial L}{\partial \dot{\beta}}$, and performing a Legendre transform yields the Hamiltonian

$$H = \frac{1}{2}(p_\alpha - n_0, p_\beta - z_0)\hat{M}^{-1}\begin{pmatrix} p_\alpha - n_0 \\ p_\beta - z_0 \end{pmatrix}. \quad (34)$$

Quantization proceeds as in the previous section, and single-valuedness of the wave function under simple gauge transformations requires that n_0 and z_0 are integers. The resulting Hamiltonian is

$$H = \frac{1}{2}(\hat{n} - n_0, \hat{z} - z_0)\hat{M}^{-1}\begin{pmatrix} \hat{n} - n_0 \\ \hat{z} - z_0 \end{pmatrix}, \quad (35)$$

where $\hat{n} \equiv -i\partial_\alpha$ and $\hat{z} \equiv -i\partial_\beta$ count the conserved number of pairs in each superfluid. Energies are obtained by replacing these number operators by their eigenvalues, i.e.,

$$\varepsilon_{n,z} = \frac{1}{2a}(n - n_0)^2 + \frac{1}{2b}(z - z_0)^2 + \frac{1}{c}(n - n_0)(z - z_0). \quad (36)$$

Here, the constants $1/a$, $1/b$, and $1/c$ are the diagonal and off-diagonal entries of \hat{M}^{-1} , respectively. One sees that all even-even nuclei in an entire region are connected via pairing, and the spectrum is an elliptical paraboloid; any section of this paraboloid is a pairing rotational band, and the sections are not limited to keeping neutron or proton numbers fixed.

It is interesting to use the isospin projection $T = n + z$ and mass number $A = 2(n + z)$ as independent variables (and similarly introduce T_0 and A_0). Then the spectrum (36) becomes

$$\varepsilon(T, A) = \left(\frac{1}{2a} + \frac{1}{2b} - \frac{1}{c}\right)\left(\frac{T - T_0}{2}\right)^2 + \left(\frac{1}{2a} + \frac{1}{2b} + \frac{1}{c}\right)\left(\frac{A - A_0}{4}\right)^2 + \left(\frac{1}{a} - \frac{1}{b}\right)\frac{(T - T_0)(A - A_0)}{8}. \quad (37)$$

The spectrum (36) recovers the results of Refs. [17,19,40,42]. The effective theory thus supports the recent proposal by Hinohara and Nazarewicz [10] to employ the pairing rotational tensor \hat{M}^{-1} as a model-independent indicator for pairing. Its eigenvectors are expected to point into the directions of the valley of β stability and perpendicular to it; the corresponding eigenvalues are expected to be small and large in magnitude, respectively.

The eigenstates of the Hamiltonian (35) are product states $|n, z\rangle$ that specify the number of pairs in each fluid, i.e.,

$$\begin{aligned} \hat{n}|n, z\rangle &= n|n, z\rangle, \\ \hat{z}|n, z\rangle &= z|n, z\rangle. \end{aligned} \quad (38)$$

Analogous to the case of one superfluid [see Eq. (10)] one can introduce pair removal (or pair addition) operators for each superfluid via

$$\begin{aligned} \hat{P} &= P_0 e^{-i\alpha}, \\ \hat{Q} &= Q_0 e^{-i\beta}. \end{aligned} \quad (39)$$

Thus,

$$\begin{aligned} \hat{P}|n, z\rangle &= P_0|n - 1, z\rangle, \\ \hat{Q}|n, z\rangle &= Q_0|n, z - 1\rangle. \end{aligned} \quad (40)$$

Double charge-exchange reactions are then governed by the nuclear matrix elements

$$\begin{aligned} \langle n - 1, z + 1 | \hat{P}\hat{Q}^\dagger | n, z \rangle &= P_0 Q_0^*, \\ \langle n + 1, z - 1 | \hat{P}^\dagger \hat{Q} | n, z \rangle &= P_0^* Q_0, \end{aligned} \quad (41)$$

while the transfer or removal of α particles involves the nuclear matrix elements

$$\begin{aligned} \langle n - 1, z - 1 | \hat{P}\hat{Q} | n, z \rangle &= P_0 Q_0, \\ \langle n + 1, z + 1 | \hat{P}^\dagger \hat{Q}^\dagger | n, z \rangle &= P_0^* Q_0^*. \end{aligned} \quad (42)$$

Thus, the leading-order theory of pairing predicts that four different reactions involve the same absolute squared nuclear matrix element, which is independent of n and z . As pair transfer in single superfluid systems, these are testable predictions for two coupled superfluids.

I briefly discuss subleading corrections of the Hamiltonian (35). These are in powers of $(\hat{n} - n_0)^k (\hat{z} - z_0)^l$ with $k + l = 3$. Alternatively, and with view on Eq. (37), one could also include powers $(T - T_0)^k (A - A_0)^l$. Following the steps in Sec. II A 2 that led to Eq. (15) one can also here estimate the uncertainties and finds

$$\begin{aligned} \Delta \varepsilon_{n,z_0} &\approx \frac{3|n - n_0|^3}{an_b^2}, \\ \Delta \varepsilon_{n_0,z} &\approx \frac{3|z - z_0|^3}{bz_b^2}, \\ \Delta \varepsilon(T, A_0) &\approx \frac{3}{4} \left(\frac{1}{2a} + \frac{1}{2b} - \frac{1}{c} \right) \frac{|T - T_0|^3}{\min(z_b^2, n_b^2)}, \\ \Delta \varepsilon(T_0, A) &\approx \frac{3}{32} \left(\frac{1}{2a} + \frac{1}{2b} + \frac{1}{c} \right) \frac{|A - A_0|^3}{\min(z_b^2, n_b^2)}, \end{aligned} \quad (43)$$

for pairing rotational bands in isotopes, isotones, isobars, and nuclei with the isospin projection, respectively, of the nucleus with n_0 neutron and z_0 proton pairs.

The effective field theory can also be extended to odd and to odd-odd nuclei, and one can easily write down the leading-order result. However, in practical applications, it is difficult to trace how states with nonzero spins evolve as neutron and proton numbers are changed, and this is particularly so for odd-odd nuclei. For this reason, such extensions of the theory are not pursued in this paper.

B. Adjustment of low-energy constants

As was the case for a single superfluid, one has to add the dominant contributions $E_{n_0,z_0} - S_{n_0}(\hat{n} - n_0) - S_{z_0}(\hat{z} - z_0)$ to the Hamiltonian (35) and finds the energy spectrum

$$E_{n,z} = E_{n_0,z_0} - S_{n_0}(n - n_0) - S_{z_0}(z - z_0) + \varepsilon_{n,z}. \quad (44)$$

Here, $\varepsilon_{n,z}$ is from Eq. (36) and contains the low-energy constants a , b , and c and S_{n_0} and S_{z_0} are (approximately) pair separation energies. I adjust the parameters S_{n_0} and a (and S_{z_0} and b) similarly as in the case of a single superfluid [see Eq. (32)] and use

$$\begin{aligned} S_{n_0} &= \frac{1}{2}(E_{n_0-1,z_0} - E_{n_0+1,z_0}), \\ a^{-1} &= E_{n_0+1,z_0} - 2E_{n_0,z_0} + E_{n_0-1,z_0}, \\ S_{z_0} &= \frac{1}{2}(E_{n_0,z_0-1} - E_{n_0,z_0+1}), \\ b^{-1} &= E_{n_0,z_0+1} - 2E_{n_0,z_0} + E_{n_0,z_0-1}. \end{aligned} \quad (45)$$

One more datum is needed to determine c and I choose the symmetric expression

$$\begin{aligned} c^{-1} &= \frac{1}{4}(E_{n_0+1,z_0+1} - E_{n_0+1,z_0-1} \\ &\quad + E_{n_0-1,z_0-1} - E_{n_0-1,z_0+1}). \end{aligned} \quad (46)$$

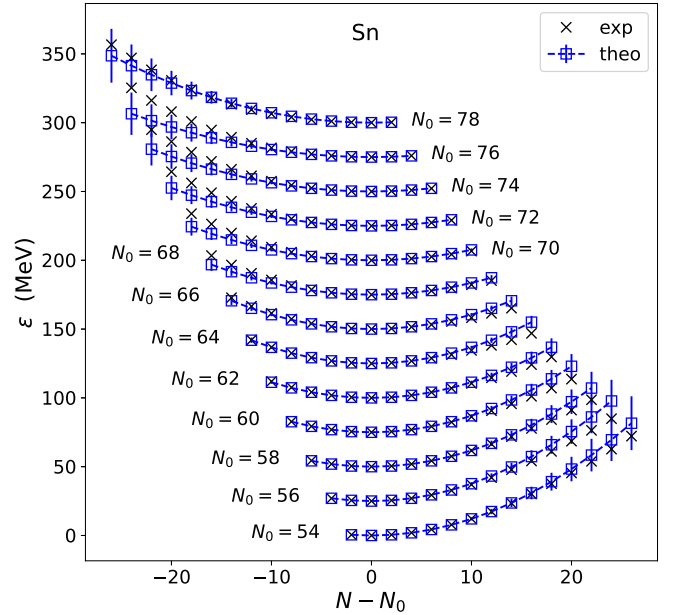


FIG. 2. Pairing rotational bands in tin isotopes, centered on nuclei with N_0 neutrons as indicated. Experimental data $E_n - E_{n_0} + S_{n_0}(n - n_0)$ is compared with the theory prediction $\varepsilon_n = (n - n_0)^2 / (2a)$ for nuclei with n pairs around n_0 . Error bars are uncertainty estimates from omitted subleading terms. Bands are shifted by multiples of 25 MeV as $N_0 = 2n_0$ is increased from 54 to 78. In each band, the energies with $|N - N_0| \leq 2$ have been adjusted to data.

IV. APPLICATIONS

A. Single superfluid: Semimagic nuclei

Figure 2 shows the pairing rotational band in tin isotopes centered on neutron number N_0 as indicated. Different bands are shifted by 25 MeV as N_0 is increased from 54 to 78. The number of pairs is $n = N/2$ and $n_0 = N_0/2$. Experimental data $E_n - E_{n_0} + S_{n_0}(n - n_0)$ are compared with the theory prediction ε_n , see Eq. (31). Here and in what follows, the y axis is simply labeled as ε . Error bars show the uncertainty estimates (16) using the average value of a from Table I. The theory describes data accurately within error bars. For each band, the three lowest-energy points with $-2 \leq N - N_0 \leq 2$ have been adjusted to data.

Figure 3 shows the pairing rotational bands in lead isotopes centered on neutron number N_0 as indicated. Different bands are shifted by 25 MeV as N_0 is increased from 98 to 122. Error bars again show the uncertainty estimates (16) using the average value of a from Table I. Theory describes data accurately within the uncertainty estimates.

Figure 4 shows the pairing rotational bands in $N = 82$ isotones centered on nuclei with proton number Z_0 as indicated. Different bands are shifted by 25 MeV as Z_0 is increased from 52 to 68. The number of pairs is $n = Z/2$ and $n_0 = Z_0/2$. Uncertainty estimates are based on Eq. (16) and the value of a from Table I. Again, theory describes data accurately within uncertainties.

In summary, the leading-order Hamiltonian (7) yields an accurate description of pairing rotational bands within

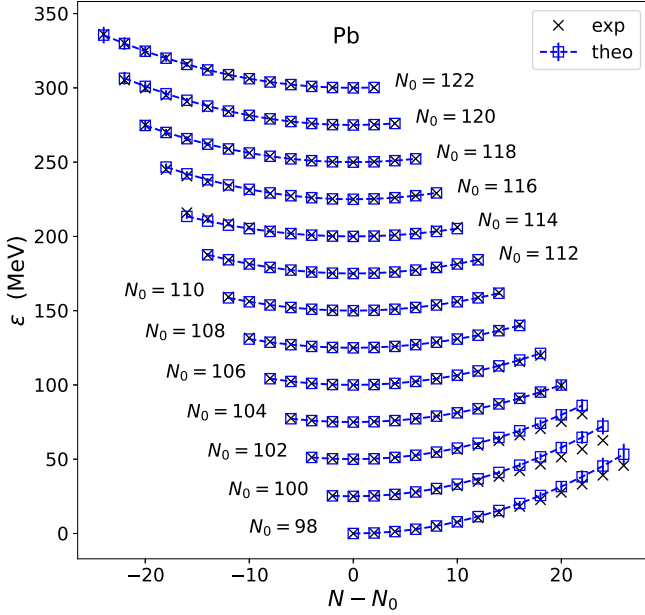


FIG. 3. Pairing rotational bands in lead isotopes centered on nuclei with neutron number N_0 as indicated. Experimental data $E_n - E_{n_0} + S_{n_0}(n - n_0)$ are compared with the theory prediction $\frac{1}{2a}(n - n_0)^2$ for nuclei with n pairs around n_0 . Error bars are uncertainty estimates for omitted subleading terms. Bands are shifted by multiples of 25 MeV as $N_0 = 2n_0$ is increased from 98 to 122. In each band, the energies with $|N - N_0| \leq 2$ have been adjusted to data.

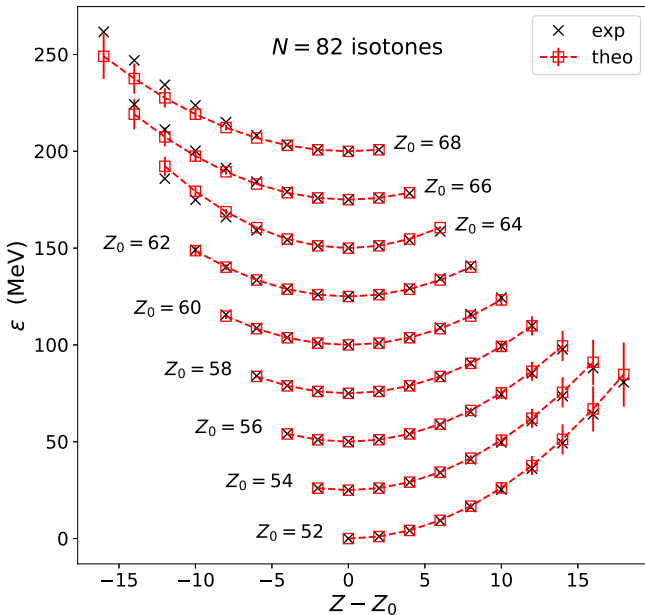


FIG. 4. Pairing rotational bands in $N = 82$ isotones, centered on nuclei with proton number Z_0 as indicated. Experimental data $E_n - E_{n_0} + S_{n_0}(n - n_0)$ are compared with the theory prediction $\frac{1}{2a}(n - n_0)^2$ for nuclei with n pairs around n_0 . Uncertainties estimate the omitted contributions from subleading terms. Bands are shifted by 25 MeV as $Z_0 = 2n_0$ is increased from 52 to 68. In each band, the energies with $|Z - Z_0| \leq 2$ have been adjusted to data.

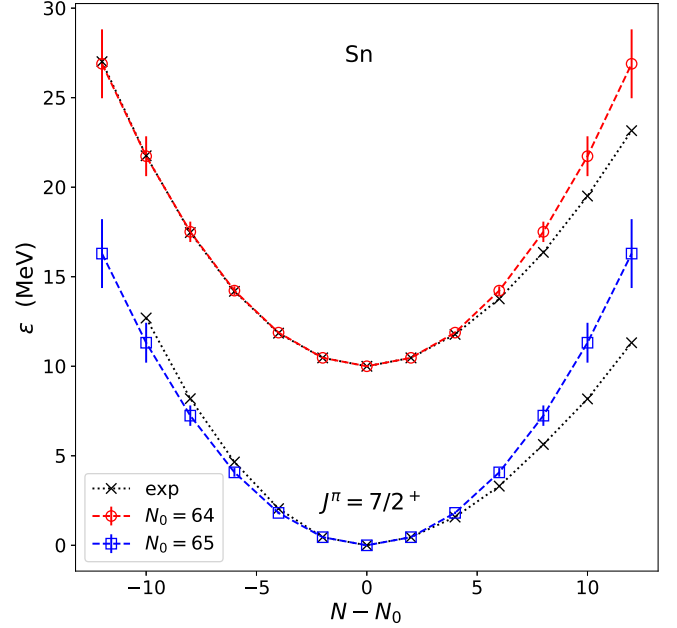


FIG. 5. Pairing rotational bands in odd (blue squares) and even (red circles) tin isotopes. The odd nuclei have spin and parity $J^\pi = 7/2^+$ with ^{115}Sn ($N_0 = 65$) at the center, while the even nuclei are centered at ^{114}Sn . Data are shown as black crosses. In each band, the central three points are adjusted to data

uncertainty estimates. This gives confidence in the power counting and the underlying separation of scales in even semimagic nuclei.

B. Odd semimagic nuclei

The ground-state spin of odd semimagic nuclei typically evolves across an isotopic or isotonic chain, and I therefore focus on low-lying states with constant spin and parity. The excitation energies of such states must be added to the ground-state energies E_n in Eq. (32) when computing the low-energy constants.

In the odd tin isotopes, the $J^\pi = 7/2^+$ state is low in energy and the pairing rotational band can be centered on the nucleus with neutron number $N_0 = 65$. The results are shown in Fig. 5 and compared with a pairing rotational band in the neighboring even isotopes (centered at $N = 64$ and shifted by 10 MeV). The uncertainty estimates (16) with a from Table I reflect the scale of deviations from data but do not capture them quantitatively for the larger values of $N - N_0$.

The agreement between theory and experiment is better in $N = 82$ isotones. In the odd isotones I focus on the $J^\pi = 5/2^+$ and $7/2^+$ states that are low in energy and can easily be traced across the chain, taking $Z = 59$ (element Pr) as the central nucleus of the pairing rotational band. The results are shown in Fig. 6 and compared with the pairing rotational band in even isotones, centered at the Nd nucleus ($Z = 60$). The uncertainty estimate (16) uses the value of a from Table I and captures the differences between theory and data.

In lead nuclei an isomeric $J^\pi = 13/2^+$ state is known in odd isotopes lighter than ^{208}Pb , although its exact spacing

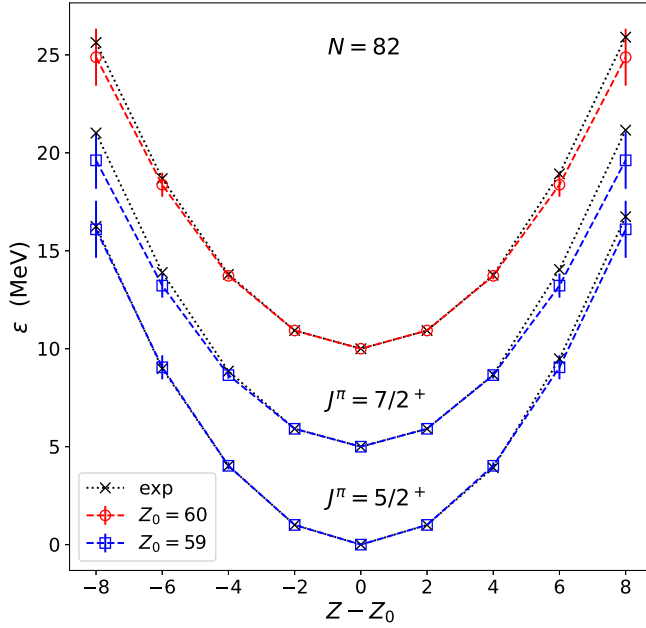


FIG. 6. Pairing rotational bands in odd (blue squares) and even (red circles) $N = 82$ isotones. Two bands connecting odd nuclei with spin and parity as indicated are centered on the Pr nucleus ($Z = 59$) and compared with the even ground-state band with the Nd nucleus ($Z = 60$) at its center. Data are shown as black crosses. In each band, the central three points are adjusted to data. Bands are shifted by multiples of 5 MeV.

with respect to the ground state is only known for ^{195}Pb and heavier isotopes; I use tentative spin assignments for more neutron-deficient isotopes and take ^{197}Pb as the center for the computation of the pairing rotational band. The results are shown in Fig. 7 and compared with an even isotope. The uncertainty estimate (16) with a from Table I captures the discrepancies between data and theory.

Overall, the results of this section show that the effective-field theory also delivers accurate results for pairing rotational bands in odd semimagic nuclei. In particular, the pairing rotational bands for even and odd semimagic nuclei have the same pairing rotational constant to a very good approximation.

C. Two superfluids: Open-shell nuclei

I take ^{166}Yb as the ($Z_0 = 70, N_0 = 96$) nucleus in the center of the rare-earth region and adjust the low-energy constants from Eqs. (45) and (46) to its immediate even-even neighbors. This yields the pairing rotational constants $1/(2a) \approx 0.30$ MeV, $1/(2b) \approx 0.94$ MeV, $1/c \approx -0.95$ MeV. The proton and neutron pairing rotational constants are consistent with those presented in Table I for Pb isotopes and $N = 82$ isotones, respectively. The size of the off-diagonal coupling $1/c$ shows that the interaction of the two superfluids is strong [10,19,43]. The curvature is small for pairing at constant isospin projection and large for isobars [see Eq. (37)].

Figure 8 shows the proton-pairing rotational bands (shifted by multiples of 12 MeV) for fixed neutron number N . Overall, theory and data agree reasonably well, and only for large

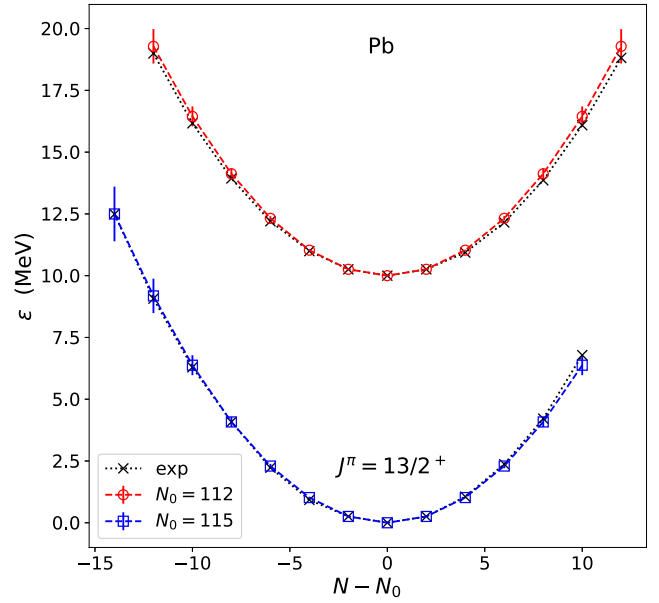


FIG. 7. Pairing rotational bands in odd (blue squares) and even (red circles) lead isotopes. The bands connecting odd nuclei with spin and parity $J^\pi = 13/2^+$ are centered on ^{197}Pb and compared with the even ground-state band with ^{112}Pb at its center. Data are shown as black crosses. In each band, the lowest three points are adjusted to data. Bands are shifted by 10 MeV.

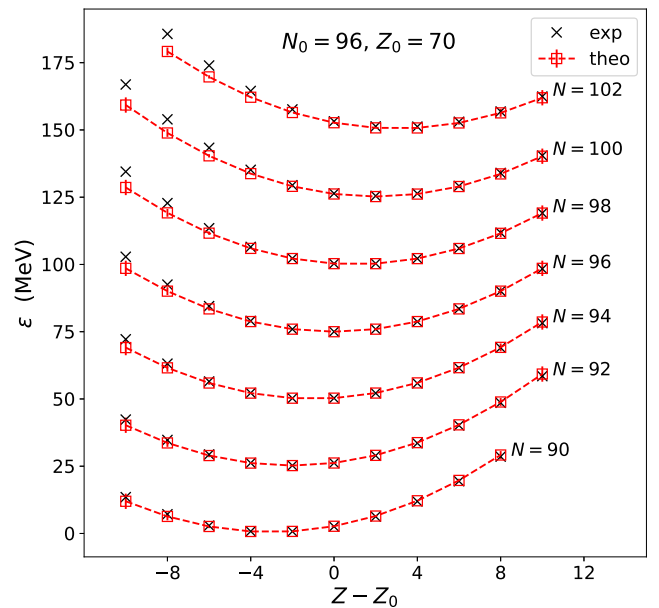


FIG. 8. Proton-pairing rotational bands as sections of a pairing elliptical paraboloid. Bands for neutron numbers as indicated in the rare-earth region around ^{166}Yb ($Z_0 = 70, N_0 = 96$). Experimental data are compared with the theory prediction. A total of six low-energy constant has been adjusted for all shown bands. Different bands are shifted by multiples of 12 MeV.

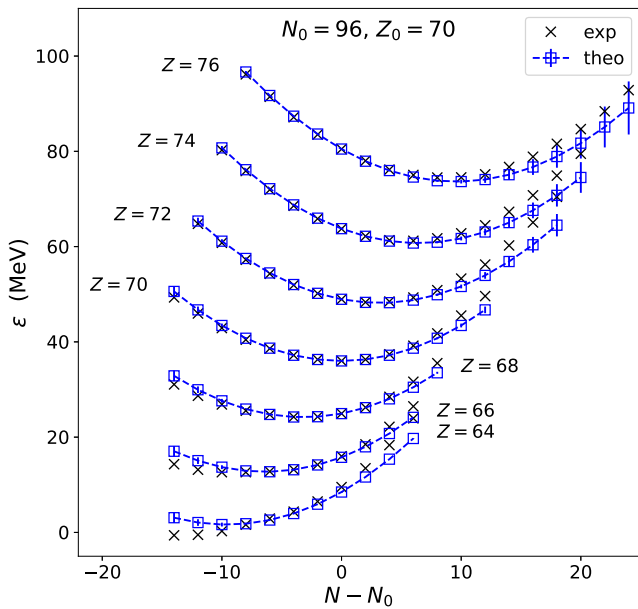


FIG. 9. Neutron-pairing rotational bands as sections of a pairing elliptical paraboloid for proton numbers as indicated in the rare-earth region around ^{166}Yb ($Z_0 = 70$, $N_0 = 96$). Experimental data are compared with the theory prediction. A total of six low-energy constant has been adjusted for all shown bands. Different bands are shifted by multiples of 12 MeV.

values of $|Z - Z_0|$, and significant away from $N = 96$ there is disagreement. The error estimates are based on $\Delta\varepsilon_{n_0,z}$ from Eqs. (43). They are too small to capture the deviations for large N and small Z .

Figure 9 shows the neutron-pairing rotational bands (shifted by multiples of 12 MeV) for fixed charge number Z . Also, here, theory describes the data fairly well, and deviations become more pronounced as $|N - N_0|$ or $|Z - Z_0|$ becomes large. The uncertainty estimates $\Delta\varepsilon_{n,z_0}$ from Eqs. (43) reflect some of the deviations but are too small for small Z .

The coupling between the two superfluids makes it interesting to also study other “directions” of pairing rotational bands [19], e.g., the isobar section and the section of constant isospin projection T_z of the pairing elliptical paraboloid (36). The former section consists of nuclei that are connected via double charge-exchange reactions, while the latter section describes nuclei that are linked by α particle capture or removal. The nucleus ^{166}Yb is kept at the center. Figure 10 shows the isobar section. Uncertainty estimates, taken as $\Delta\varepsilon(T, A_0)$ from Eqs. (43), capture the scale of the difference to data but are not quantitatively correct.

Figure 11 shows the section with constant isospin projection. Here, the uncertainties are taken as $\Delta\varepsilon(T_0, A)$ from Eqs. (43). They capture well the scale of differences between theory and data.

The comparison of the isobar and constant T_z pairing rotational bands with the $N = 96$ proton pairing band of Fig. 8 and the $Z = 70$ neutron pairing band of Fig. 9 shows that the rotational constants differ considerably for each section of

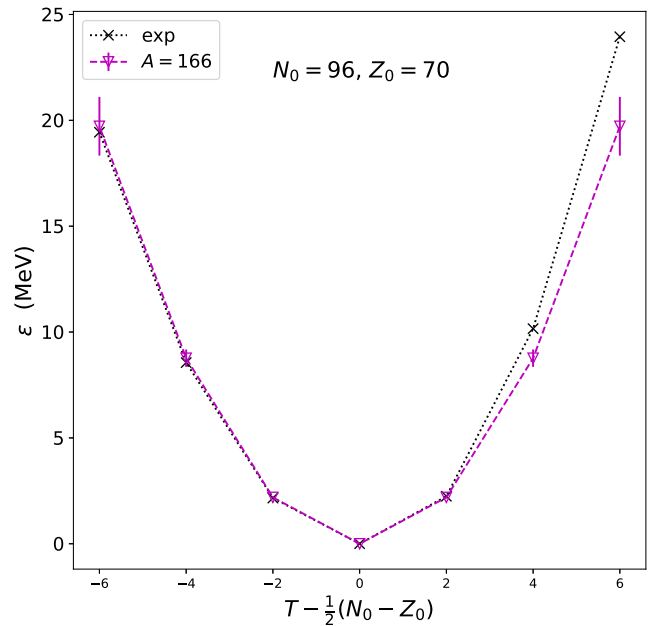


FIG. 10. Isobaric rotational band of $A = 166$ nuclei as a section of the pairing elliptical paraboloid centered at the nucleus ^{166}Yb ($Z_0 = 70$, $N_0 = 96$). Experimental data are compared with the theory prediction.

the elliptical paraboloid. Diagonalization of the mass matrix yields eigenvalues 0.09 and 2.4 MeV, and the corresponding eigenvectors have an angle of 28° and 118° with the neutron axis on the Segrè chart, respectively. (This is essentially along

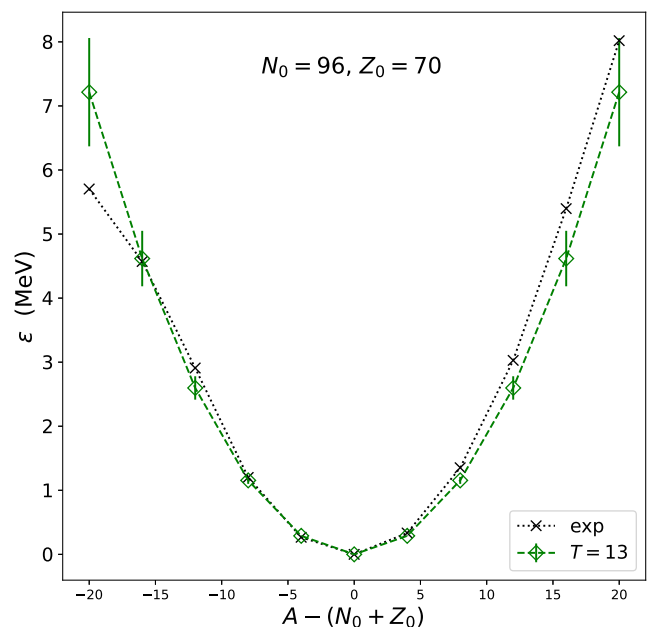


FIG. 11. Pairing rotational band with fixed isospin projection $T = 13$ as a section of the pairing elliptical paraboloid centered at the nucleus ^{166}Yb ($Z_0 = 70$, $N_0 = 96$). Experimental data are compared with the theory prediction.

the valley of β stability and perpendicular to it.) Consistent with this, the neutron pairing bands and the constant- T_z pairing band have the smallest curvature because they are oriented mainly along the valley of β stability.

D. Estimating energy gains from particle number projection

There is another interesting application of Eq. (44). Calculations based on nuclear energy density functionals [44,45] or Hamiltonians [46,47] often do not employ particle number projections. Then, one really computes a symmetry-breaking state (with a fixed orientation in gauge space), which consists of a superposition of states with different numbers of pairs. Such a localized state clearly has too much kinetic energy in gauge space, and the formula (36) allows one to estimate this. Using $\langle \hat{N} \rangle = N_0$ and $\Delta N^2 \equiv \langle (\hat{N} - N_0)^2 \rangle$, and similar for \hat{Z} , one finds

$$\Delta E = \frac{1}{8a} \langle \Delta N^2 \rangle + \frac{1}{8b} \langle \Delta Z^2 \rangle + \frac{1}{4c} \langle \Delta N \Delta Z \rangle. \quad (47)$$

Here, the coefficients a , b , and c may be determined from computations or data via Eqs. (45) and (46).

As an example, I take the computation of semimagic ^{64}Ni within Bogoliubov many-body perturbation theory in Ref. [48]. The number variance is about $\Delta N^2 \approx 16$ (see Fig. 9 of that work), and $(2a)^{-1} \approx 0.72$ MeV [from data using Eq. (32)]. This yields $\Delta E \approx 2.9$ MeV.

V. SUMMARY

This paper revisited pairing rotations in a model-independent way within an effective field theory. It followed the standard approach to emergent symmetry breaking via a nonlinear realization of the broken phase symmetry. This led to pairing rotational bands in semimagic nuclei and to a pairing elliptical paraboloid in systems where paired protons and neutrons interact. Coupling a fermion to the superfluid extends the theory to odd semimagic nuclei. The expansion of the effective Hamiltonians is in powers of differences of Cooper-pair numbers, and subleading corrections are suppressed by inverse powers of the maximum number of pairs in a shell. The key input for the effective field theory consists of the matrix containing the pairing rotational constants. The eigenvalues of this model-independent quantity are given by the curvatures of the nuclear ground-state energies as a function of proton and neutron numbers. A comparison with data shows that the leading-order theory is accurate (within uncertainty estimates) for heavy semimagic nuclei and for nuclei sufficiently far away from shell closures.

The theory predicts that pair transfer is constant for nuclei in a pairing rotational band. For nuclei on a pairing elliptical paraboloid, the nuclear matrix element for pair transfer, double charge-exchange reactions, and α particle knockout or capture are nucleus independent and related to each other.

It is interesting to compare the effective theory of this work with the those for deformed nuclei [27,39,49–51]. For axially symmetric deformations, one exploits the emergent symmetry breaking of rotational SO(3) down to axial SO(2). Then the coset spaces is the two-sphere and Nambu-Goldstone modes parametrize that manifold. Finite ground-state spins and fermions introduce couplings to gauge potentials (which usually are referred to as Coriolis forces). The treatment of pairing is technically somewhat simpler than deformation because the broken-symmetry groups are Abelian. Otherwise, however, one follows the same path.

One could combine both approaches, simultaneously capturing deformation and superfluidity. Then, the low-energy physics of nuclei away from shell closures becomes extremely simple: The pattern of the emergent symmetry breaking—from a product of rotational SO(3) times pairing $U(1) \times U(1)$ down to axial SO(2)—is all that matters. The symmetries are realized nonlinearly, and low-lying excitations are the quantized excitations of the corresponding Nambu-Goldstone modes in finite systems. Each nucleus exhibits a ground-state rotational band and pairing rotations connect ground-state energies of different nuclei. While there are, of course, many nuclear models that break symmetries or incorporate the effects of symmetry breaking, the effective field theory approach makes it front and center, is aware about its breakdown scale, and allows one to make systematic improvements and uncertainty estimates.

ACKNOWLEDGMENTS

This work has been supported by the U.S. Department of Energy under Grant No. DE-FG02-96ER40963 and under Contract No. DE-AC05-00OR22725 with UT-Battelle, LLC (Oak Ridge National Laboratory). This manuscript has been authored by UT-Battelle, LLC under Contract No. DE-AC05-00OR22725 with the U.S. Department of Energy. The U.S. Government retains and the publisher, by accepting the article for publication, acknowledges that the U.S. Government retains a non-exclusive, paid-up, irrevocable, world-wide license to publish or reproduce the published form of this manuscript, or allow others to do so, for U.S. Government purposes. The Department of Energy will provide public access to these results of federally sponsored research in accordance with the DOE Public Access Plan [52].

-
- [1] A. Bohr, B. R. Mottelson, and D. Pines, Possible analogy between the excitation spectra of nuclei and those of the superconducting metallic state, *Phys. Rev.* **110**, 936 (1958).
 [2] A. B. Migdal, Superfluidity and the moments of inertia of nuclei, *Nucl. Phys.* **13**, 655 (1959).
 [3] D. R. Bès and R. A. Broglia, Pairing vibrations, *Nucl. Phys.* **80**, 289 (1966).

- [4] Y. Nogami, Improved superconductivity approximation for the pairing interaction in nuclei, *Phys. Rev.* **134**, B313 (1964).
 [5] A. Bohr, Pair correlations and double transfer reactions, in *Nuclear Structure: Dubna Symposium 1968 (Dubna, 4-11 July 1968)*, Proceedings Series (International Atomic Energy Agency, Vienna, 1969), p. 179.

- [6] D. R. Bès, R. A. Broglia, R. P. J. Perazzo, and K. Kumar, Collective treatment of the pairing Hamiltonian: (I). Formulation of the model, *Nucl. Phys. A* **143**, 1 (1970).
- [7] R. A. Broglia, O. Hansen, and C. Riedel, Two-neutron transfer reactions and the pairing model, in *Advances in Nuclear Physics*, edited by M. Baranger and E. Vogt (Springer, Boston, 1973), Vol. 6, Chap. 3, p. 287.
- [8] D. M. Brink and R. A. Broglia, *Nuclear Superfluidity: Pairing in Finite Systems*, Cambridge Monographs on Particle Physics, Nuclear Physics and Cosmology (Cambridge University Press, Cambridge, UK, 2005).
- [9] R. A. Broglia, J. Terasaki, and N. Giovanardi, The Anderson–Goldstone–Nambu mode in finite and in infinite systems, *Phys. Rep.* **335**, 1 (2000).
- [10] N. Hinohara and W. Nazarewicz, Pairing Nambu–Goldstone Modes within Nuclear Density Functional Theory, *Phys. Rev. Lett.* **116**, 152502 (2016).
- [11] G. Potel, A. Idini, F. Barranco, E. Vigezzi, and R. A. Broglia, From bare to renormalized order parameter in gauge space: Structure and reactions, *Phys. Rev. C* **96**, 034606 (2017).
- [12] W. von Oertzen and A. Vitturi, Pairing correlations of nucleons and multi-nucleon transfer between heavy nuclei, *Rep. Prog. Phys.* **64**, 1247 (2001).
- [13] G. Potel, F. Barranco, F. Marini, A. Idini, E. Vigezzi, and R. A. Broglia, Calculation of the Transition from Pairing Vibrational to Pairing Rotational Regimes between Magic Nuclei ^{100}Sn and ^{132}Sn via Two-Nucleon Transfer Reactions, *Phys. Rev. Lett.* **107**, 092501 (2011).
- [14] G. Potel, A. Idini, F. Barranco, E. Vigezzi, and R. A. Broglia, Cooper pair transfer in nuclei, *Rep. Prog. Phys.* **76**, 106301 (2013).
- [15] G. Potel, A. Idini, F. Barranco, E. Vigezzi, and R. A. Broglia, Quantitative study of coherent pairing modes with two-neutron transfer: Sn isotopes, *Phys. Rev. C* **87**, 054321 (2013).
- [16] H. Shimoyama and M. Matsuo, Anomalous pairing vibration in neutron-rich Sn isotopes beyond the $N = 82$ magic number, *Phys. Rev. C* **84**, 044317 (2011).
- [17] R. Beck, M. Kleber, and H. Schmidt, Pairing rotations and separation energies, *Z. Phys. A: Hadrons Nucl.* **250**, 155 (1972).
- [18] M. Matsuo, Treatment of nucleon-number conservation in the selfconsistent collective-coordinate method: Coupling between large-amplitude collective motion and pairing rotation, *Prog. Theor. Phys.* **76**, 372 (1986).
- [19] N. Hinohara, Collective inertia of the Nambu–Goldstone mode from linear response theory, *Phys. Rev. C* **92**, 034321 (2015).
- [20] N. Hinohara, Extending pairing energy density functional using pairing rotational moments of inertia, *J. Phys. G* **45**, 024004 (2018).
- [21] T. Kouno, C. Ishizuka, T. Inakura, and S. Chiba, Pairing strength in the relativistic mean-field theory determined from the fission barrier heights of actinide nuclei and verified by pairing rotation and binding energies, *Prog. Theor. Exp. Phys.* **2022**, 023D02 (2021).
- [22] U. Van Kolck, Effective field theory of nuclear forces, *Prog. Part. Nucl. Phys.* **43**, 337 (1999).
- [23] H.-W. Hammer and R. J. Furnstahl, Effective field theory for dilute Fermi systems, *Nucl. Phys. A* **678**, 277 (2000).
- [24] P. F. Bedaque and U. van Kolck, Effective field theory for few-nucleon systems, *Annu. Rev. Nucl. Part. Sci.* **52**, 339 (2002).
- [25] R. J. Furnstahl, H.-W. Hammer, and S. J. Puglia, Effective field theory for dilute fermions with pairing, *Ann. Phys. (NY)* **322**, 2703 (2007).
- [26] E. Epelbaum, H.-W. Hammer, and Ulf-G. Meißner, Modern theory of nuclear forces, *Rev. Mod. Phys.* **81**, 1773 (2009).
- [27] T. Papenbrock, Effective theory for deformed nuclei, *Nucl. Phys. A* **852**, 36 (2011).
- [28] H. W. Griedhammer, J. A. McGovern, D. R. Phillips, and G. Feldman, Using effective field theory to analyse low-energy Compton scattering data from protons and light nuclei, *Prog. Part. Nucl. Phys.* **67**, 841 (2012).
- [29] H.-W. Hammer, C. Ji, and D. R. Phillips, Effective field theory description of halo nuclei, *J. Phys. G* **44**, 103002 (2017).
- [30] H.-W. Hammer, S. König, and U. van Kolck, Nuclear effective field theory: Status and perspectives, *Rev. Mod. Phys.* **92**, 025004 (2020).
- [31] M. R. Schindler and D. R. Phillips, Bayesian methods for parameter estimation in effective field theories, *Ann. Phys. (NY)* **324**, 682 (2009).
- [32] R. J. Furnstahl, D. R. Phillips, and S. Wesolowski, A recipe for EFT uncertainty quantification in nuclear physics, *J. Phys. G* **42**, 034028 (2015).
- [33] J. Gasser and H. Leutwyler, Spontaneously broken symmetries: Effective Lagrangians at finite volume, *Nucl. Phys. B* **307**, 763 (1988).
- [34] C. Yannouleas and U. Landman, Symmetry breaking and quantum correlations in finite systems: Studies of quantum dots and ultracold Bose gases and related nuclear and chemical methods, *Rep. Prog. Phys.* **70**, 2067 (2007).
- [35] S. Weinberg, Nonlinear realizations of chiral symmetry, *Phys. Rev.* **166**, 1568 (1968).
- [36] C. G. Callan, S. Coleman, J. Wess, and B. Zumino, Structure of phenomenological Lagrangians. II, *Phys. Rev.* **177**, 2247 (1969).
- [37] S. Coleman, J. Wess, and B. Zumino, Structure of phenomenological Lagrangians. I, *Phys. Rev.* **177**, 2239 (1969).
- [38] T. Brauner, Spontaneous symmetry breaking and Nambu–Goldstone bosons in quantum many-body systems, *Symmetry* **2**, 609 (2010).
- [39] T. Papenbrock and H. A. Weidenmüller, Effective field theory for finite systems with spontaneously broken symmetry, *Phys. Rev. C* **89**, 014334 (2014).
- [40] H. J. Krappe, On the use of a variable moment of pairing, *Z. Phys. A: Hadrons Nucl.* **275**, 297 (1975).
- [41] T. Kishimoto and T. Kammuri, Pair rotation in the dynamical nuclear field theory, *Prog. Theor. Phys.* **74**, 1245 (1985).
- [42] E. R. Marshalek, The RPA at high spin and conservation laws, *Nucl. Phys. A* **275**, 416 (1977).
- [43] X. B. Wang, J. Dobaczewski, M. Kortelainen, L. F. Yu, and M. V. Stoitsov, Lipkin method of particle-number restoration to higher orders, *Phys. Rev. C* **90**, 014312 (2014).
- [44] M. Bender, Paul-Henri Heenen, and Paul-Gerhard Reinhard, Self-consistent mean-field models for nuclear structure, *Rev. Mod. Phys.* **75**, 121 (2003).
- [45] T. Nikšić, D. Vretenar, and P. Ring, Relativistic nuclear energy density functionals: Mean-field and beyond, *Prog. Part. Nucl. Phys.* **66**, 519 (2011).
- [46] W. H. Dickhoff and C. Barbieri, Self-consistent Green’s function method for nuclei and nuclear matter, *Prog. Part. Nucl. Phys.* **52**, 377 (2004).

- [47] V. Somà, C. Barbieri, and T. Duguet, Ab initio Gorkov-Green's function calculations of open-shell nuclei, *Phys. Rev. C* **87**, 011303(R) (2013).
- [48] A. Tichai, R. Roth, and T. Duguet, Many-body perturbation theories for finite nuclei, *Front. Phys.* **8** (2020).
- [49] Q. B. Chen, N. Kaiser, Ulf-G. Meißner, and J. Meng, Effective field theory for triaxially deformed nuclei, *Eur. Phys. J. A* **53**, 204 (2017).
- [50] T. Papenbrock and H. A. Weidenmüller, Effective field theory for deformed odd-mass nuclei, *Phys. Rev. C* **102**, 044324 (2020).
- [51] I. K. Afnamlah, E. A. Coello Pérez, and D. R. Phillips, Effective field theory approach to rotational bands in odd-mass nuclei, *Phys. Rev. C* **104**, 064311 (2021).
- [52] <http://energy.gov/downloads/doe-public-access-plan>.